Capacity Enhancement of Band-Limited DS-CDMA System Using Weighted Despreading Function

Yuejin Huang, *Member, IEEE,* and Tung-Sang Ng, *Senior Member, IEEE*

***Abstract*— This paper addresses capacity enhancement of a band-limited direct-sequence code-division multiple-access system by using a weighted despreading function (WDF) in the receiver. An ideal Gaussian channel with perfect power control is assumed. The system performance is measured by the signal-to-interference-plus-noise ratio of the decision variable derived in the frequency domain, the bandwidth efficiency factor, the capacity enhancement factor, and the bit-error rate. It is shown that tuning a parameter of the WDF employed helps to partially flatten the in-band cross-spectrum of a pair of spreading and despreading functions. Numerical results show that the capacity of the proposed system improves over the conventional system using rectangular despreading function. To assess practical implications of the WDF receiver, the sensitivity to timing error is also analyzed.**

***Index Terms*— Band-limited systems, cellular bandwidth efficiency, direct-sequence code-division multiple access, weighted despreading function.**

I. Introduction

In A direct-sequence code-division multiple-access (DS-CDMA) system, a major limitation to system capacity is due to multiple-access interference (MAI). To increase system capacity, several techniques have been proposed for MAI rejection, e.g., multiuser detection [1]–[4] and noise whitening technique at the symbol level [5], [6] or chip level [7]–[10]. These techniques improve system performance significantly because of the assumption of infinite bandwidth or knowledge of other user information. In a band-limited DS-CDMA system, a critical consideration on system design is how to efficiently use a given bandwidth. It has been shown that the spreading signals with flat power spectral density (PSD) across the bandwidth will yield the optimal performance [11]. For example, in the IS-95 standard, each of the chip pulses of a spreading signal is shaped to be approximately a Sinc function to achieve the flat in-band spectrum. The cost is the complicated production of the pulses because of each pulse's long duration in the time domain. When spreading signals with nonflat spectrum are used in practice, different techniques can be employed in the receiver to compensate for the in-band PSD of the received nonflat spectrum signals, for example, the prewhitening filter in [7] and [8] and the system with polar nonreturn-to-zero signaling and Manchester signaling in [12]. In [9], a receiver (single-user detector) with weighted despreading functions (WDF's) was proposed for MAI rejection. The technique can be considered as an approximation to the optimal noise-whitening receiver (ONWR) [7] and the performance analysis was done under the assumption that system bandwidth is infinite. Comparing with the ONWR, the WDF receiver can be built and adjusted easily. The potential to partially whiten the in-band PSD of the received colored signals and hence to improve the system performance in band-limited scenario was also hinted at in [9]. It is currently an open problem to derive the optimum solution for the finite bandwidth case.

In this paper, we extend the work in [9] to band-limited signals. In our approach, the transmitted signals are generated by passing square-wave spreading signals through an analog low-pass filter. Such a transmitter is simple and can operate at high chip rates. By using the proposed WDF in the receiver, it will be shown that the in-band cross PSD of a pair of spreading and corresponding WDF's can be flattened by simply tuning a parameter of the WDF. As a result, system performance improves especially when the additive white Gaussian noise (AWGN) is insignificant. If there is no constraint on system bandwidth, we will show that more improvement on the system performance can be obtained by tuning the WDF parameter as the bandwidth increases. When the bandwidth extends to infinity, the system performance coincides with the results derived in [9]. Further, to assess practical implications, the sensitivity to timing error of the proposed receiver is analyzed.

The rest of the paper is organized as follows. Section II describes the system model. In Section III, the signal-to-interference-plus-noise ratio (SINR) of the decision variable for a band-limited DS-CDMA system is derived in the frequency domain when the WDF is employed. This is followed by numerical results in Section IV. Analysis of sensitivity to timing error is given in Section V and finally, in Section VI, conclusions are given.

II. System Model

Suppose there are K CDMA users accessing the channel. The transmitter for the kth user is shown in Fig. 1(a). The

Paper approved by U. Mitra, the Editor for Spread Spectrum/Equalization of the IEEE Communications Society. Manuscript received December 1, 1997; revised June 30, 1998 and February 2, 1999. This work was supported by the Hong Kong Research Grants Council and the CRCG of the University of Hong Kong.

Y. Huang was with the Department of Electrical and Electronic Engineering, University of Hong Kong, Hong Kong. He is now with the Department of Electrical and Computer Engineering, McGill University, Montreal, PQ H3A 2A7 Canada (e-mail: yjhuang@wireless.ece.mcgill.ca).

T.-S. Ng is with the Department of Electrical and Electronic Engineering, University of Hong Kong, Hong Kong (e-mail: tsng@eee.hku.hk).

Publisher Item Identifier S 0090-6778(99)06300-X.

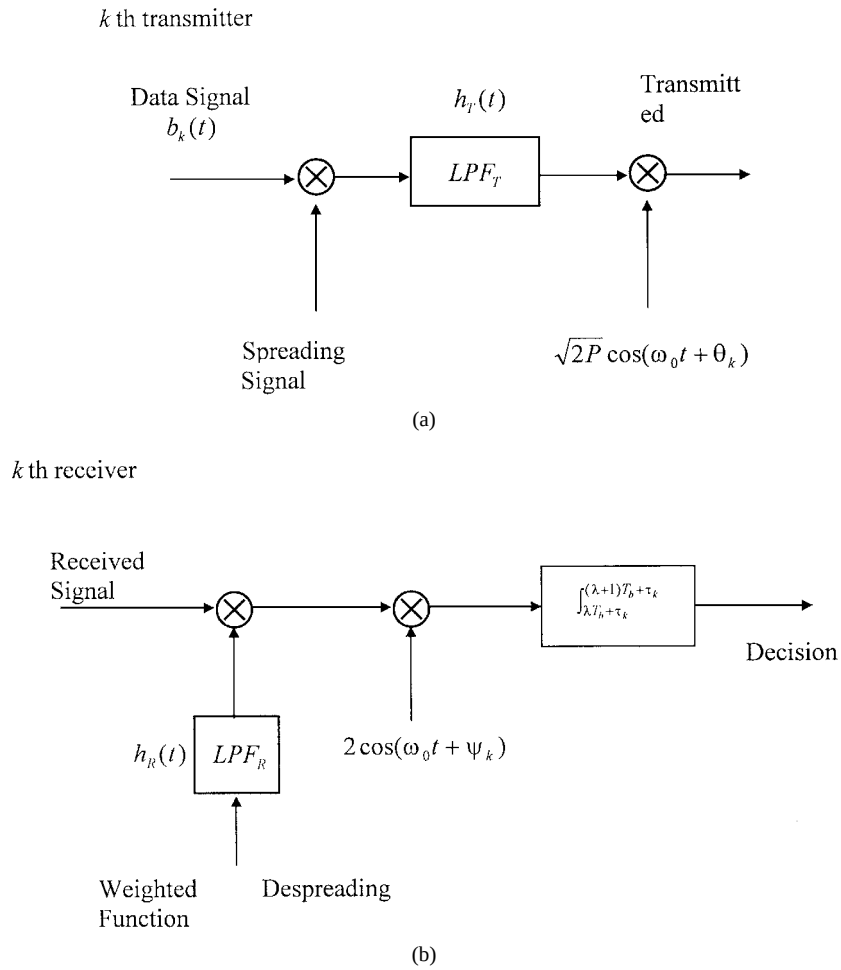

Fig. 1. System model for the kth transceiver: (a) transmitter and (b) receiver.

transmitted binary data signal $b_k(t)$ is first multiplied by a spreading signal $a_k(t)$ with phase synchronized to $b_k(t)$ to spread each data bit. Then the spreading signal with data information is passed through an analog low-pass filter LPF_T with impulse response $h_T(t)$ to limit the out-of-band emissions. The output signal of LPF_T is used to modulate a carrier at f_0, thus producing a BPSK modulated signal. The spreading and data signals for the kth user are given by $a_k(t) = \sum_{j=-\infty}^{\infty} a_j^{(k)} P_{T_c}(t - jT_c)$ and $b_k(t) = \sum_{j=-\infty}^{\infty} b_j^{(k)} P_{T_b}(t - jT_b)$, where T_c and T_b are chip and bit duration, respectively, and $P_x(y) = 1$ for $0 < y < x$ and $P_x(y) = 0$, otherwise. In our study, $b_j^{(k)}$ and $a_j^{(k)}$ are modeled as independent random variables taking values -1 or $+1$ with equal probabilities. It is assumed that there are N chips of a spreading sequence in the interval of each data bit T_b and the spreading sequence is a random binary sequence. The transmitted signal for the kth user is

$$S_k(t) = \sqrt{2P}[v_k(t) * h_T(t)] \cos(\omega_0 t + \theta_k) \tag{1}$$

where $v_k(t) = b_k(t)a_k(t)$ and "$*$" denotes convolution. The transmitted power P and the carrier frequency ω_0 are common to all users. The parameter θ_κ is the phase of the kth user.

In a Gaussian channel with perfect power control, the received signal $r(t)$ at the input of a receiver is given by

$$\begin{aligned} r(t) &= \sum_{k=1}^{K} S_k(t - \tau_k) + n(t) \\ &= \sum_{k=1}^{K} \sqrt{2P}[v_k(t - \tau_k) * h_T(t - \tau_k)] \\ &\quad \cdot \cos(\omega_0 t + \psi_k) + n(t) \end{aligned} \tag{2}$$

where K is the number of active users, $\psi_k (= \theta_k - \omega_0 \tau_k)$ is random phase uniformly distributed on $[0, 2\pi]$, and $n(t)$ is AWGN with two-side PSD $N_0/2$.

For BPSK modulation, the structure of the kth receiver is shown in Fig. 1(b). In the receiver, there is an analog low-pass filter LPF_R with impulse response $h_R(t)$ placed between the WDF and the multiplier [13]. For the purpose of whitening the spectrum of received colored MAI signals, the receiver is designed to have the impulse response matched to $2[\hat{a}_k(t) * h_R(t)] \cos(\omega_0 t) P_{T_b}(t)$ where $\hat{a}_k(t)$[1] is the WDF with details given below. To simplify the notation, an analog

[1]It has been pointed out by an anonymous reviewer that $\hat{a}_i(t)$ can be obtained by passing $a(t)$ through a filter $h_r(t) = -(1-L(\epsilon))/2\delta(t+T\Delta) + \delta(t) - (1-L(\epsilon))/2\delta(t-T\Delta)$.

bandpass filter between the input signal and the multiplier is ignored because its effects on signal-to-interference ratio (SIR) can be merged into those of the transmitter filter $h_T(t)$. The WDF for the user k's receiver can be expressed as [9]

$$\hat{a}_k(t) = \sum_{j=-\infty}^{\infty} a_j^{(k)} w_j^{(k)}\left(t - jT_c \middle| \left\{c_j^{(k)}, c_{j+1}^{(k)}\right\}\right) \quad (3)$$

where $c_j^{(k)} = a_{j-1}^{(k)} a_j^{(k)}$; and $w_j^{(k)}(t|\{c_j^{(k)}, c_{j+1}^{(k)}\})$ for $0 \le t \le T_c$ is the jth chip weighting waveform for the kth receiver conditioned on the status of three consecutive chips $\{c_j^{(k)}, c_{j+1}^{(k)}\} = \{a_{j-1}^{(k)} a_j^{(k)}, a_j^{(k)} a_{j+1}^{(k)}\}$. The jth conditioned chip weighting waveform for the kth user is defined as [9, eq. (5)]

$$w_j^{(k)}\left(t \middle| \left\{c_j^{(k)}, c_{j+1}^{(k)}\right\}\right) = \begin{cases} m_1(t) & \text{if } c_j^{(k)} = +1 \text{ and } c_{j+1}^{(k)} = +1 \\ m_2(t) & \text{if } c_j^{(k)} = -1 \text{ and } c_{j+1}^{(k)} = -1 \\ m_3(t) & \text{if } c_j^{(k)} = -1 \text{ and } c_{j+1}^{(k)} = +1 \\ m_4(t) & \text{if } c_j^{(k)} = +1 \text{ and } c_{j+1}^{(k)} = -1 \end{cases} \quad (4)$$

with the elements of the chip weighting waveform vector $\{m_1(t), m_2(t), m_3(t), m_4(t)\}$ selected as [9, eq. (7)]

$$\begin{aligned} m_1(t) &= L(\varepsilon) P_{T_c}(t) \\ m_2(t) &= P_{T_c}(t) - [1 - L(\varepsilon)] P_{T_c - 2T_\Delta}(t - T_\Delta) \\ m_3(t) &= P_{T_\Delta}(t) + L(\varepsilon) P_{T_c - T_\Delta}(t - T_\Delta) \\ m_4(t) &= L(\varepsilon) P_{T_c - T_\Delta}(t) + P_{T_c}(t) - P_{T_c - T_\Delta}(t) \end{aligned} \quad (5)$$

where $T_\Delta \in (0, T_c/2]$, $\varepsilon = T_c/T_\Delta \in [2, \infty)$ is a parameter of the chip weighting waveforms, $L(\varepsilon)$ is a monotonically decreasing function of ε and is defined as $L(\varepsilon) = [C(\varepsilon - 2) + 1]^{-1}$. The constant C is chosen equal to 6.3 in this study to minimize the effect of timing error on performance and will be further explained in Section V. When $\varepsilon = 2$ in (5), the chip weighting waveforms $\{m_p(t)\}_{p=1}^4$ reduce to the rectangular pulse $P_{T_c}(t)$. The chip weighting waveforms can be found in [9, Fig. 2(b)].

III. Performance Analysis

A. Signal-to-Interference-Plus-Noise Ratio

We arbitrarily choose the ith user as the desired user and analyze the SINR performance of the proposed receiver for data symbol $b_\lambda^{(i)}$. After the filter with the impulse response matched to $2[\hat{a}_i(t) * h_R(t)] \cos(\omega_0 t + \psi_i) P_{T_b}(t)$, the conditional output random variable of the ith user receiver, denoted by $\zeta_i(\lambda)$, can be expressed as

$$\zeta_i(\lambda) = \int_{\lambda T_b + \tau_i}^{(\lambda+1)T_b + \tau_i} 2r(t)[\hat{a}_i(t - \lambda T_b - \tau_i) * h_R(t - \lambda T_b - \tau_i)] \cdot \cos(\omega_0 t + \psi_i)\, dt \quad (6)$$

where $\cos(\omega_0 t + \psi_i)$ is the coherent carrier reference of the desired user and $\hat{a}_i(t - \lambda T_b - \tau_{il})$ is the WDF for the λth bit of the desired user. Since the carrier frequency f_0 is much larger than T_b^{-1} in a practical system, the double-frequency terms in (6) can be ignored. Then (6) is reduced to

$$\zeta_i(\lambda) = S_i^{(\lambda)}(\varepsilon) + N_i(\lambda) + \sum_{k=1, k\ne i}^{K} I_{k,i} \quad (7)$$

where the first, second, and third components are the desired, noise, and MAI components which are described in detail below. According to (6), the desired signal term $S_i^{(\lambda)}(\varepsilon)$ in (7) can be expressed as

$$S_i^{(\lambda)}(\varepsilon) = \sqrt{2P} \int_0^{T_b} [v_i(t + \lambda T_b) * h_T(t + \lambda T_b)] \cdot [\hat{a}_i(t) * h_R(t)]\, dt. \quad (8)$$

From (6), the noise term $N_i(\lambda)$ in (7) can be expressed as

$$N_i(\lambda) = \int_0^{T_b} [n_c(t) \cos\psi_i - n_s(t) \sin\psi_i][\hat{a}_i(t) * h_R(t)]\, dt \quad (9)$$

where the terms $n_c(t)$ and $n_s(t)$ are low-pass equivalent components of the AWGN $n(t)$. In the third component of (7), the term $I_{k,i}$ is given by

$$I_{k,i} = \sqrt{2P} \cos(\psi_i - \psi_k) \int_0^{T_b} [v_k(t + \tau_i - \tau_k) * h_T(t + \tau_i - \tau_k)] \cdot [\hat{a}_i(t) * h_R(t)]\, dt. \quad (10)$$

To express the SINR in the frequency domain, we assume that the processing gain N is so large that the characteristic of all sub-sequences of length N for each user can be represented approximately by the average characteristic of the sequence employed. To simplify the notation, we also assume that the two analog low-pass filters LPF_T and LPF_R in the transmit-receive chain are identical and have the same frequency response $H(f)$. Then, following the approach used in [13], (8) can be expressed in the form

$$S_i^{(\lambda)}(\varepsilon) = \sqrt{2P} T_b \int_{-\infty}^{\infty} S_{a\hat{a}}(f, \varepsilon) |H(f)|^2\, df \quad (11)$$

where $S_{a\hat{a}}(f, \varepsilon)$, with a parameter ε, is the cross PSD of a pair of spreading and WDF's. Also, using a similar derivation in [13], the variance of the white noise term $N_i(\lambda)$, denoted by $\sigma_N^2(\varepsilon)$, can be represented as

$$\sigma_N^2(\varepsilon) = N_0 T_b \int_{-\infty}^{\infty} S_{\hat{a}\hat{a}}(f, \varepsilon) |H(f)|^2\, df \quad (12)$$

where $S_{\hat{a}\hat{a}}(f, \varepsilon)$ is the PSD of the WDF. The variance of the MAI term $\sum_{k=1, k\ne i}^{K} I_{k,i}$ in (7), denoted by $\sigma_I^2(\varepsilon)$, can be expressed as [13]

$$\sigma_I^2(\varepsilon) = P T_b (K - 1) \int_{-\infty}^{\infty} S_{aa}(f) S_{\hat{a}\hat{a}}(f, \varepsilon) |H(f)|^4\, df \quad (13)$$

where $S_{aa}(f)$ is the PSD of the spreading function. By definition, the SINR is given by

$$\mathrm{SINR}(\varepsilon) = \left(\frac{\sigma_N^2(\varepsilon)}{\left[S_i^{(\lambda)}(\varepsilon)\right]^2} + \frac{\sigma_I^2(\varepsilon)}{\left[S_i^{(\lambda)}(\varepsilon)\right]^2} \right)^{-1} \quad (14)$$

where $S_i^{(\lambda)}(\varepsilon)$, $\sigma_N^2(\varepsilon)$, and $\sigma_I^2(\varepsilon)$ are given by (11)–(13), respectively. For clarity, (14) is rewritten in the form

$$\mathrm{SINR}(\varepsilon) = \left(\frac{1}{\mathrm{SNR}(\varepsilon)} + \frac{1}{\mathrm{SIR}(\varepsilon)}\right)^{-1} \tag{15}$$

where

$$\mathrm{SNR}(\varepsilon) = \frac{2E_b}{N_0} \cdot \frac{\left(\int_{-\infty}^{\infty} S_{a\hat{a}}(f,\varepsilon)|H(f)|^2\,df\right)^2}{\int_{-\infty}^{\infty} S_{\hat{a}\hat{a}}(f,\varepsilon)|H(f)|^2\,df} \tag{16}$$

and

$$\mathrm{SIR}(\varepsilon) = \frac{2T_b}{K-1} \cdot \frac{\left(\int_{-\infty}^{\infty} S_{a\hat{a}}(f,\varepsilon)|H(f)|^2\,df\right)^2}{\int_{-\infty}^{\infty} S_{aa}(f) S_{\hat{a}\hat{a}}(f,\varepsilon)|H(f)|^4\,df}. \tag{17}$$

B. Cross- and Auto-Power Spectra

In order to obtain the cross PSD, we first evaluate the cross-correlation function $R_{a\hat{a}}(t,\tau,\varepsilon)$ of an arbitrary spreading function $a_k(t)$ and its corresponding WDF $\hat{a}_k(t)$. By definition, we obtain

$$R_{a\hat{a}}(t,\tau,\varepsilon) \equiv E\{a_k(t)\hat{a}_k(t-\tau)\}. \tag{18}$$

Using (3), (18) becomes

$$\begin{aligned} R_{a\hat{a}}(t,\tau,\varepsilon) = E\Bigg\{ & \sum_{j=-\infty}^{\infty}\sum_{m=-\infty}^{\infty} a_j^{(k)} a_m^{(k)} w_m^{(k)} \\ & \cdot \left(t-\tau-mT_c \middle| \left\{c_m^{(k)}, c_{m+1}^{(k)}\right\}\right) \\ & \cdot P_{T_c}(t-jT_c)\Bigg\} \end{aligned} \tag{19}$$

where $\{c_m^{(k)}, c_{m+1}^{(k)}\} = \{a_{m-1}^{(k)} a_m^{(k)}, a_m^{(k)} a_{m+1}^{(k)}\}$. Because $a_j^{(k)}$ is independent of $a_m^{(k)} w_m^{(k)}(t-\tau-mT_c|\{c_m^{(k)}, c_{m+1}^{(k)}\})$ when $|m-j|>1$, (19) reduces to

$$\begin{aligned} & R_{a\hat{a}}(t,\tau,\varepsilon) \\ & = \sum_{j=-\infty}^{\infty} w_j^{(k)}\left(t-\tau-jT_c \middle| \left\{c_j^{(k)}, c_{j+1}^{(k)}\right\}\right) P_{T_c}(t-jT_c) \\ & \quad + \sum_{j=-\infty}^{\infty} c_j^{(k)} w_{j-1}^{(k)}\left(t-\tau-jT_c+T_c \middle| \left\{c_{j-1}^{(k)}, c_j^{(k)}\right\}\right) \\ & \quad \cdot P_{T_c}(t-jT_c) \\ & \quad + \sum_{j=-\infty}^{\infty} c_{j+1}^{(k)} w_{j+1}^{(k)}\left(t-\tau-jT_c-T_c \middle| \left\{c_{j+1}^{(k)}, c_{j+2}^{(k)}\right\}\right) \\ & \quad \cdot P_{T_c}(t-jT_c). \end{aligned} \tag{20}$$

The cross-correlation function $R_{a\hat{a}}(t,\tau,\varepsilon)$ depends on t as well as on τ. Note that a time shift changes the phases of the components of a waveform but does not affect its power spectrum. We can evaluate the cross PSD, denoted by $S_{a\hat{a}}(f,\varepsilon)$, by assuming the time variable t in (20) is a random time shift uniformly distributed in $[0, T_c]$ [14]. Thus, we can simply average (20) over the time shift and obtain the cross-correlation function with a parameter ε by using (4), which is independent of the time variable t

$$\begin{aligned} R_{a\hat{a}}(\tau,\varepsilon) = {} & \frac{1}{4T_c}\sum_{p=1}^{4}\int_0^{T_c} m_p(t-\tau)\,dt + \frac{1}{4T_c} \\ & \cdot \sum_{p=1}^{4}(-1)^{p-1}\int_0^{T_c} m_p(t-\tau+T_c)\,dt \end{aligned} \tag{21}$$

for $\tau \geq 0$. Substituting (5) into (21), we obtain

$$\begin{aligned} & R_{a\hat{a}}(\tau,\varepsilon) \\ & = \begin{cases} \dfrac{1+(\varepsilon-1)L(\varepsilon)}{\varepsilon} - \dfrac{\tau}{T_c}, & 0 \leq \tau \leq \dfrac{T_c}{\varepsilon} \\ L(\varepsilon)\left[\dfrac{T_c-\tau}{T_c}\right], & \dfrac{T_c}{\varepsilon} \leq \tau \leq T_c - \dfrac{T_c}{\varepsilon} \\ \dfrac{(\varepsilon+1)L(\varepsilon)+(\varepsilon-1)}{2\varepsilon} & \\ \quad -\dfrac{[L(\varepsilon)+1]\tau}{2T_c}, & T_c - \dfrac{T_c}{\varepsilon} \leq \tau \leq T_c \\ \dfrac{(\varepsilon+1)L(\varepsilon)-(\varepsilon+1)}{2\varepsilon} & \\ \quad -\dfrac{[L(\varepsilon)-1]\tau}{2T_c}, & T_c \leq \tau \leq T_c + \dfrac{T_c}{\varepsilon} \\ 0, & T_c + \dfrac{T_c}{\varepsilon} \leq \tau\ . \end{cases} \end{aligned} \tag{22}$$

Since $R_{a\hat{a}}(\tau,\varepsilon) = R_{a\hat{a}}(-\tau,\varepsilon)$, the cross PSD $S_{a\hat{a}}(f,\varepsilon)$ is the Fourier transform of (22) with respect to τ, viz.

$$\begin{aligned} & S_{a\hat{a}}(f,\varepsilon) \\ & = 2\int_0^{\infty} R_{a\hat{a}}(\tau,\varepsilon)\cos(2\pi f\tau)\,d\tau \\ & = \left(\frac{1}{4\pi^2 f^2 T_c}\right)\Bigg\{\Bigg[2\cos\left(\frac{2\pi f T_c}{\varepsilon}\right) - \cos\left(\frac{2\pi f T_c(\varepsilon-1)}{\varepsilon}\right) \\ & \qquad - \cos\left(\frac{2\pi f T_c(\varepsilon+1)}{\varepsilon}\right)\Bigg] L(\varepsilon) \\ & \qquad + \Bigg[\cos\left(\frac{2\pi f T_c(\varepsilon+1)}{\varepsilon}\right) + 2 - 2\cos\left(\frac{2\pi f T_c}{\varepsilon}\right) \\ & \qquad - 2\cos(2\pi f T_c) + \cos\left(\frac{2\pi f T_c(\varepsilon-1)}{\varepsilon}\right)\Bigg]\Bigg\}. \end{aligned} \tag{23}$$

The PSD of the spreading function $a_k(t)$, denoted by $S_{aa}(f)$, is easily shown to be

$$S_{aa}(f) = S_{a\hat{a}}(f,2) = \frac{1-\cos(2\pi f T_c)}{2\pi^2 f^2 T_c}. \tag{24}$$

Similar to the derivation of (23), the PSD $S_{\hat{a}\hat{a}}(f, \varepsilon)$ of the WDF is given by

$$\begin{aligned}
&S_{\hat{a}\hat{a}}(f,\varepsilon)\\
&=\left(\frac{1}{8T_c\pi^2 f^2}\right)\left\{\left[2\cos\left(\frac{4\pi fT_c}{\varepsilon}\right)-\cos\left(\frac{2\pi fT_c(\varepsilon+2)}{\varepsilon}\right)\right.\right.\\
&\qquad+2-\cos\left(\frac{2\pi fT_c(\varepsilon-2)}{\varepsilon}\right)\\
&\qquad\left.-2\cos(2\pi fT_c)\right]L^2(\varepsilon)+\left[-4\cos\left(\frac{4\pi fT_c}{\varepsilon}\right)\right.\\
&\qquad+2\cos\left(\frac{2\pi fT_c(\varepsilon+2)}{\varepsilon}\right)-4\\
&\qquad+2\cos\left(\frac{2\pi fT_c(\varepsilon-2)}{\varepsilon}\right)\\
&\qquad-4\cos\left(\frac{2\pi fT_c(\varepsilon-1)}{\varepsilon}\right)\\
&\qquad+4\cos(2\pi fT_c)+8\cos\left(\frac{2\pi fT_c}{\varepsilon}\right)\\
&\qquad\left.-4\cos\left(\frac{2\pi fT_c(\varepsilon+1)}{\varepsilon}\right)\right]L(\varepsilon)\\
&\qquad+\left[6-8\cos\left(\frac{2\pi fT_c}{\varepsilon}\right)\right.\\
&\qquad+2\cos\left(\frac{4\pi fT_c}{\varepsilon}\right)-\cos\left(\frac{2\pi fT_c(\varepsilon+2)}{\varepsilon}\right)\\
&\qquad-6\cos(2\pi fT_c)-\cos\left(\frac{2\pi fT_c(\varepsilon-2)}{\varepsilon}\right)\\
&\qquad+4\cos\left(\frac{2\pi fT_c(\varepsilon+1)}{\varepsilon}\right)\\
&\qquad\left.\left.+4\cos\left(\frac{2\pi fT_c(\varepsilon-1)}{\varepsilon}\right)\right]\right\}. \qquad (25)
\end{aligned}$$

After some algebraic manipulation, it can be proved that

$$S^2_{a\hat{a}}(f,\varepsilon)=S_{aa}(f)S_{\hat{a}\hat{a}}(f,\varepsilon). \qquad (26)$$

Substituting (23)–(25) into (15), we obtain the system SINR(ε) which is a function of ε and K (the number of active users). For a given K, tuning ε leads to maximization of SINR(ε). Clearly, the expression of SINR(ε) is too complex to be tuned adaptively for different K in a practical situation. However, when K is large or when the system is operating near capacity, the AWGN is negligible and the optimal SNR(ε) performance can be achieved by a fixed ε [see (28) and Fig. 4].

C. Bandwidth Efficiency Factor $F_{BE}(\varepsilon, B)$

To simplify the performance analysis of the band-limited CDMA system, we assume that the two analog low-pass filters LPF_T and LPF_R are ideal low-pass filters with frequency response given by

$$H(f)=\begin{cases}1, & |f|\le B\\ 0, & |f|>B\end{cases} \qquad (27)$$

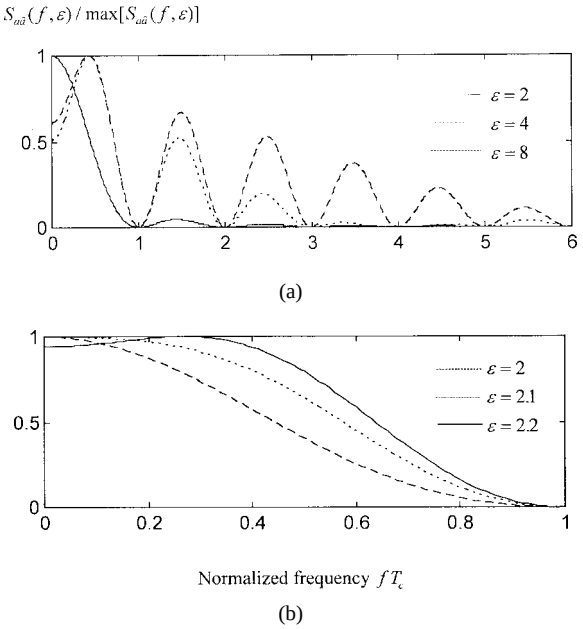

Fig. 2. The normalized cross spectrum $S_{a\hat{a}}(f, \varepsilon)/\max[S_{a\hat{a}}(f, \varepsilon)]$ versus fT_c with ε as a parameter: (a) fT_c from zero to six and (b) ft_c from zero to one.

where B is the system bandwidth. Thus, substituting (27) into (17) and using (26), we can rewrite the SIR(ε) as

$$\mathrm{SIR}(\varepsilon)=\frac{4BT_b}{K-1}F_{BE}(\varepsilon, B) \qquad (28)$$

where

$$F_{BE}(\varepsilon, B)=\frac{1}{2B}\cdot\frac{\left(\int_{-B}^{B}S_{a\hat{a}}(f,\varepsilon)\,df\right)^2}{\int_{-B}^{B}S^2_{a\hat{a}}(f,\varepsilon)\,df} \qquad (29)$$

is referred to as the bandwidth efficiency factor [12]. For a CDMA system operating near capacity, the AWGN is usually insignificant when compared with the MAI, so that the system performance relies only on SIR(ε) and hence $F_{BE}(\varepsilon, B)$. Clearly, when the cross-PSD $S_{a\hat{a}}(f, \varepsilon)$ is a constant across the bandwidth B, $F_{BE}(\varepsilon, B)$ can reach its maximum value of one. To illustrate the effects of ε on in-band PSD, we plot the normalized cross spectrum $S_{a\hat{a}}(f, \varepsilon)/\max[S_{a\hat{a}}(f, \varepsilon)]$ against normalized frequency fT_c (from zero to six) for three values of ε in Fig. 2(a). Note that the WDF employed reduces to a rectangular spreading function at $\varepsilon = 2$, and the solid curve in the figure represents the cross PSD of a conventional receiver. From these curves, we also observe that the relative strength of the cross PSD at high frequency becomes larger as ε increases. Fig. 2(b) shows the normalized cross PSD versus normalized frequency fT_c (from zero to one) for three values of ε. Clearly, assuming that the system bandwidth is equal to the chip rate, the in-band $S_{a\hat{a}}(f, \varepsilon)$ can be partially flattened by tuning ε.

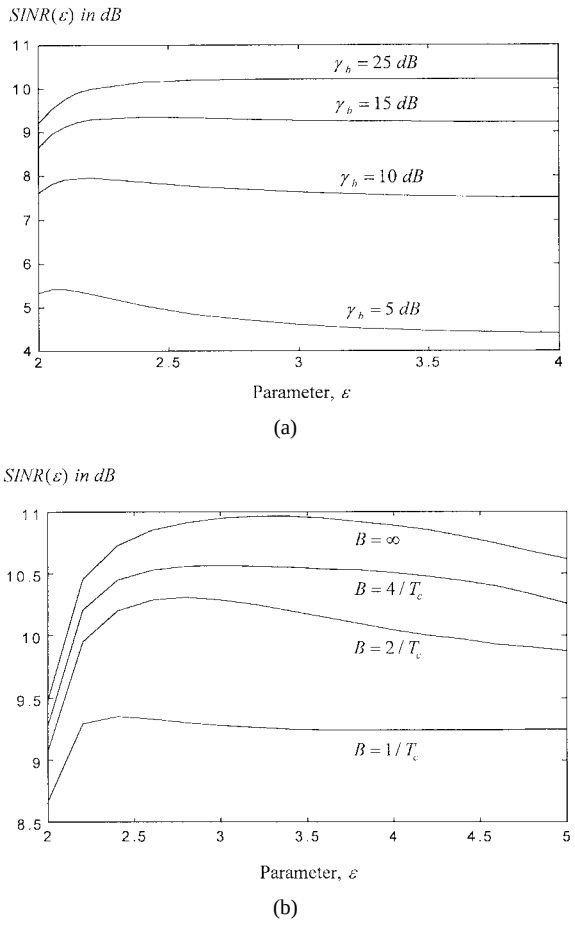

Fig. 3. System SINR(ε) against ε when $N = 255$ and $K = 75$: (a) SINR for $B = 1/T_c$ with γ_b as a parameter and (b) SINR for $\gamma_b = 15$ dB with B as a parameter.

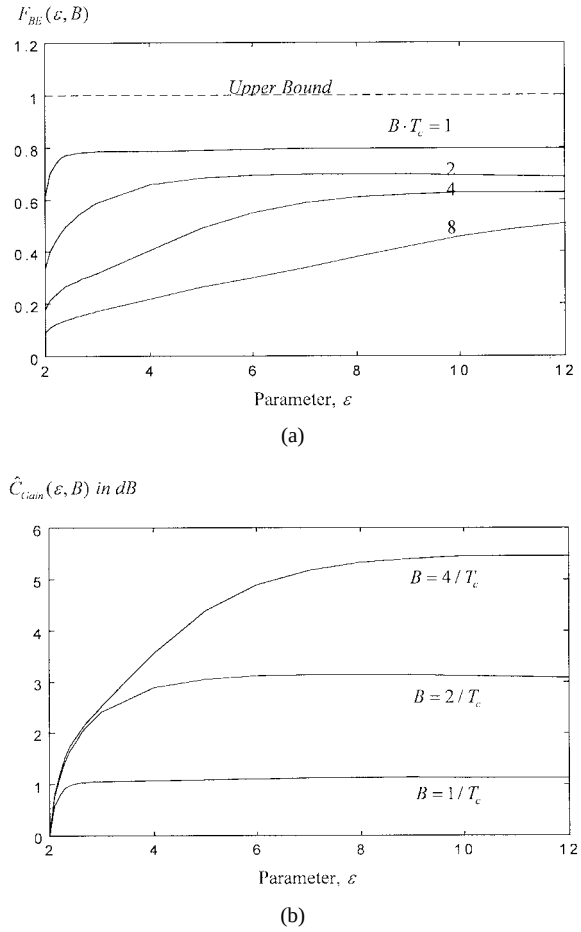

Fig. 4. Two factors versus ε with bandwidth B as a parameter: (a) bandwidth efficiency factor $F_{BE}(\varepsilon, B)$ and (b) capacity enhancement factor $\hat{C}_{\text{Gain}}(\varepsilon, B)$.

For the purpose of performance comparison between the proposed and the conventional receivers, we define the capacity enhancement factor $\hat{C}_{\text{Gain}}(\varepsilon, B)$ in decibels, as

$$\hat{C}_{\text{Gain}}(\varepsilon, B) = 10 \log_{10} \left[\frac{F_{BE}(\varepsilon, B)}{F_{BE}(2, B)} \right] \tag{30}$$

which is also a function of ε and B. Notice that $F_{BE}(2, B)$ is the bandwidth efficiency factor for the conventional CDMA receiver with $\varepsilon = 2$.

IV. Numerical Results

In the following, $N = 255$, $K = 75$, and $H(f)$ given by (27) are used when either the SINR or the bit-error rate (BER) performance are evaluated. For the BER evaluation, Gaussian assumption is used as K and N are large.

Let us first consider the SINR performance. Upon using (15) with $H(f)$ given by (27), we plot in Fig. 3(a) the system SINR(ε) versus ε with $B = 1/T_c$ and using $\gamma_b = E_b/N_0$ as a parameter. Note that the values of SINR(2) for different γ_b represent the SINR performance of a conventional receiver with rectangular despreading function. From this figure, one can see that the SINR performance of the proposed receiver can be improved by tuning ε, but the amount of the improvement is limited due to the bandwidth constraint of $B = 1/T_c$. For example, the increased SINR by tuning ε is about 1 dB at $\gamma_b = 25$ dB. From this figure, it is also clear that the gap between curves with $\gamma_b = 5$ dB and $\gamma_b = 15$ dB is much larger than that between the curves with $\gamma_b = 15$ dB and $\gamma_b = 25$ dB. This indicates that the system SINR increases as γ_b increases when the AWGN is significant. On the other hand, when the MAI dominates over the AWGN (large γ_b), the SINR gain with the same increase of γ_b is relatively small. To show the effect of bandwidth on system SINR, we plot the SINR(ε) versus ε for different values of B at a fixed $\gamma_b = 15$ dB in Fig. 3(b). Clearly at the γ_b considered and for a given bandwidth B, SINR(ε) can be optimized by tuning ε. It is also clear from the graphs that the increase in SINR(ε) by tuning ε is far greater than the conventional receiver ($\varepsilon = 2$) for the same increase of bandwidth. This implies that the conventional receiver, from the point of view of bandwidth efficiency, becomes less effective as the bandwidth increases. Although increase in bandwidth continues to improve the performance of the proposed receiver, the returns become marginal after $B > 4/T_c$ at the given γ_b.

Next we consider the bandwidth efficiency factor $F_{BE}(\varepsilon, B)$ [given by (29)] which is a measure of performance of a band-limited CDMA system operating near capacity. Fig. 4(a) plots $F_{BE}(\varepsilon, B)$ versus ε for four values of B. From

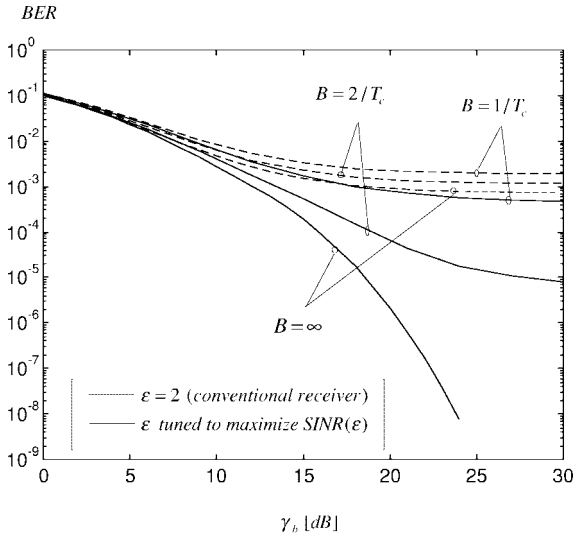

Fig. 5. BER performance versus γ_b for three values of bandwidth B when $N = 255$ and $K = 75$.

this figure, one can see that the bandwidth efficiency factor at $B = 1/T_c$ is always larger than that at higher bandwidth. This figure also shows that at a given bandwidth, $F_{BE}(\varepsilon, B)$ can be increased just by tuning ε, e.g., $F_{BE}(2, 1/T_c) = 0.613$, $F_{BE}(3, 1/T_c) = 0.783$, and $F_{BE}(12, 1/T_c) = 0.7944$, etc. Note that $F_{BE}(2, 1/T_c) = 0.613$ is the bandwidth efficiency factor for the conventional receiver when $B = 1/T_c$. As a result, the SIR(ε) is also increased because SIR(ε) given by (28) is proportional to the factor $F_{BE}(\varepsilon, B)$. In Fig. 4(b), the capacity enhancement factor $\hat{C}_{\text{Gain}}(\varepsilon, B)$ is plotted against ε with bandwidth B as a parameter. In contrast with $F_{BE}(\varepsilon, B)$, $\hat{C}_{\text{Gain}}(\varepsilon, B)$ increases as B increases. The graphs indicate the use of WDF in a receiver can provide substantial improvement over the conventional receiver ($\varepsilon = 2$). In the case when the bandwidth is constrained to satisfy $B = 1/T_c$, the factor $\hat{C}_{\text{Gain}}(\varepsilon, B)$ can be increased up to about 1 dB by tuning ε.

Finally, let us consider the BER performance of the proposed receiver. The error probability P_e is defined as $P_e = Q(\sqrt{\text{SINR}(\varepsilon)})$ where $Q(x) = (2\pi)^{-1} \int_x^\infty \exp(-t^2/2)\, dt$. Fig. 5 shows the BER performance of both the proposed and the conventional receivers versus γ_b for three cases of bandwidth. At a given bandwidth, the improved BER is obvious when using the WDF in the receiver. The curves in Fig. 5 also show clearly that the improved BER of the proposed receiver is much larger when compared with the conventional receiver for the same increase in bandwidth. From this figure, it is also apparent that the BER performance of the proposed receiver can be improved without floor when system bandwidth is infinite. On the other hand, the increased performance of the conventional receiver is limited even though system bandwidth extends to infinity.

V. Sensitivity to Timing Error

In previous sections, all the results are obtained with the assumption that no timing error exists. However, to assess whether the improved performance is practically achievable or

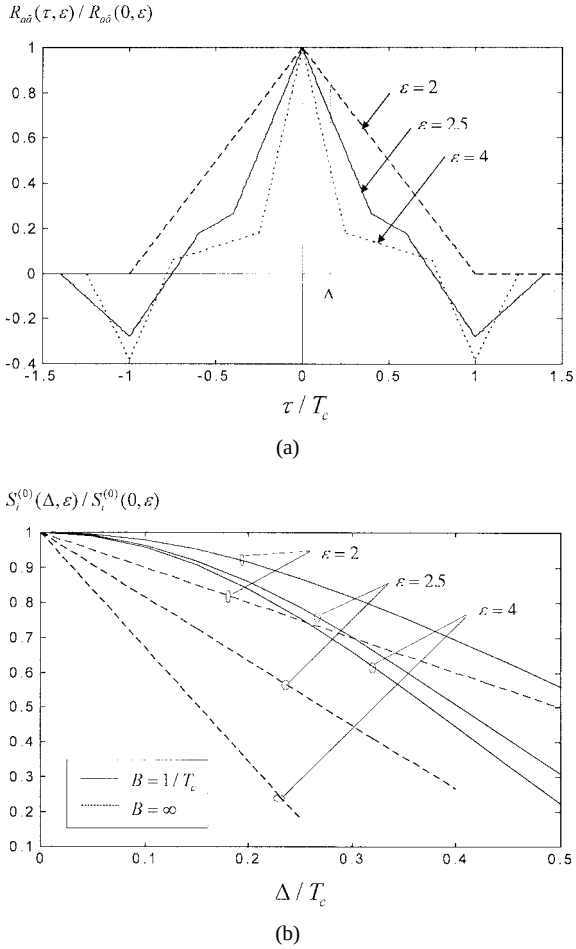

Fig. 6. Normalized cross-correlation function and desired signal strength with ε as a parameter: (a) normalized cross-correlation function $R_{a\hat{a}}(\tau, \varepsilon)/R_{a\hat{a}}(0, \varepsilon)$ and (b) normalized desired signal strength $S_i^{(0)}(\Delta, \varepsilon)/S_i^{(0)}(0, \varepsilon)$ for two values of B.

not, it is important to evaluate the relative sensitivity to timing error for both the proposed and the conventional receivers. For this purpose, we plot the normalized cross-correlation function $\rho(\tau, \varepsilon) = R_{a\hat{a}}(\tau, \varepsilon)/R_{a\hat{a}}(0, \varepsilon)$ for three values of ε when $B = \infty$ in Fig. 6(a) where $R_{a\hat{a}}(\tau, \varepsilon)$ is given by (22). Note that $R_{a\hat{a}}(\tau, 2)$ corresponds to the cross-correlation function of the conventional receiver. As the relative strength of the desired signal in the decision variable depends only on the value of $\rho(\tau, \varepsilon)$ at sampling instances, it is apparent that the proposed receiver is more sensitive to timing error than the conventional receiver as ε increases. For example, at the sampling instant of $0.1T_c$, $\rho(0.1T_c, 2) = 0.9$, $\rho(0.1T_c, 2.5) = 0.8146$, and $\rho(0.1T_c, 4) = 0.6723$. In other words, when the system bandwidth is infinite, the performance degradation of the proposed receiver due to the same timing error Δ is much greater than that of the conventional receiver.

We now analyze a band-limited system as follows. From (8), the desired signal term with timing error Δ for the zeroth bit, denoted by $S_i^{(0)}(\Delta, \varepsilon)$, can be expressed in the form

$$S_i^{(0)}(\Delta, \varepsilon) = \sqrt{2P} \int_0^{T_b} [v_i(t) * h_T(t)] \cdot [\hat{a}_i(t - \Delta) * h_R(t - \Delta)]\, dt. \quad (31)$$

Assuming that $b_0^{(i)} = 1$, (31) becomes

$$\begin{aligned} S_i^{(0)}(\Delta,\varepsilon) =& \sqrt{2P}\int_0^{T_b}[a_i(t) * h_T(t)] \\ & \cdot [\hat{a}_i(t-\Delta) * h_R(t-\Delta)]\,dt \\ =& \sqrt{2P}\int_{-\infty}^{\infty}\int_{-\infty}^{\infty}\left(\int_0^{T_b} a_i(t-\tau)\hat{a}_i(t-\Delta-\xi)\,dt\right) \\ & \cdot h_T(\tau)h_R(\xi)\,d\tau\,d\xi. \end{aligned} \tag{32}$$

For large processing gain N, (32) can be approximately represented by the ensemble cross-correlation function [13]. Therefore, we obtain

$$\begin{aligned} S_i^{(0)}(\Delta,\varepsilon) &= \sqrt{2P}T_b[R_{a\hat{a}}(\tau,\varepsilon) * h_T(\tau) * h_R(\tau)]_{\tau=\Delta} \\ &= \sqrt{2P}T_b\int_{-\infty}^{\infty} S_{a\hat{a}}(f,\varepsilon)H_T(f)H_R(f)e^{j2\pi f\Delta}\,df. \end{aligned} \tag{33}$$

Since $H_T(f) = H_R(f) = H(f)$ given by (27) and $S_{a\hat{a}}(f,\varepsilon) = S_{a\hat{a}}(-f,\varepsilon)$, (33) becomes

$$S_i^{(0)}(\Delta,\varepsilon) = 2\sqrt{2P}T_b\int_0^B S_{a\hat{a}}(f,\varepsilon)\cos(2\pi f\Delta)\,df. \tag{34}$$

Clearly

$$\rho(\Delta,\varepsilon) = \lim_{B\to\infty}\left[S_i^{(0)}(\Delta,\varepsilon)\Big/S_i^{(0)}(0,\varepsilon)\right]. \tag{35}$$

To illustrate the effects of bandwidth on the degradation of desired signal strength due to timing error Δ, we plot normalized desired signal strength $S_i^{(0)}(\Delta,\varepsilon)/S_i^{(0)}(0,\varepsilon)$ against the timing error Δ with ε as a parameter in Fig. 6(b) for the cases of $B = 1/T_c$ and $B = \infty$. It is apparent that degradation in $S_i^{(0)}(\Delta,\varepsilon)/S_i^{(0)}(0,\varepsilon)$ due to timing error becomes more serious with increasing bandwidth and increasing ε.

To show the increased SINR at a given Δ by using WDF in the receiver, we define the SINR gain in decibels as

$$G_{\mathrm{SINR}}(\Delta,\varepsilon) = 10\log_{10}[\mathrm{SINR}(\Delta,\varepsilon)] - 10\log_{10}[\mathrm{SINR}(\Delta,2)] \tag{36}$$

where $\mathrm{SINR}(\Delta,\varepsilon)$ denotes the SINR of the decision variable at a given Δ and ε. Clearly, $\mathrm{SINR}(\Delta,2)$ is the SINR of the conventional receiver with timing error Δ. Replacing $S_i^{(\lambda)}(\varepsilon)$ in (14) by (34), the SINR for the zeroth bit at a given Δ can be represented as

$$\mathrm{SINR}(\Delta,\varepsilon) = \frac{\left[S_i^{(0)}(\Delta,\varepsilon)\right]^2}{\sigma^2(\varepsilon)} = \mathrm{SINR}(0,\varepsilon)\frac{\left[S_i^{(0)}(\Delta,\varepsilon)\right]^2}{\left[S_i^{(0)}(0,\varepsilon)\right]^2} \tag{37}$$

where $\sigma^2(\varepsilon) = \sigma_N^2(\varepsilon) + \sigma_I^2(\varepsilon)$ is independent of Δ and $\mathrm{SINR}(0,\varepsilon)$ is equal to the $\mathrm{SINR}(\varepsilon)$ defined by (14). Substituting (37) into (36), we obtain

$$G_{\mathrm{SINR}}(\Delta,\varepsilon) = G_{\mathrm{SINR}}(0,\varepsilon) - 20\log_{10}\left[\frac{S_i^{(0)}(\Delta,2)\Big/S_i^{(0)}(0,2)}{S_i^{(0)}(\Delta,\varepsilon)\Big/S_i^{(0)}(0,\varepsilon)}\right] \tag{38}$$

where $G_{\mathrm{SINR}}(0,\varepsilon)$ is the SINR gain by using the WDF in the receiver when no timing error exists and $S_i^{(0)}(\Delta,\varepsilon)$ is given by (34). According to Fig. 3(a), $G_{\mathrm{SINR}}(0,\varepsilon)$ is about 1 dB when $B = 1/T_c$, $N = 255$, $K = 75$, $\gamma_b = 25$ dB, and $\varepsilon \geq 2.5$. Assuming $G_{\mathrm{SINR}}(0,\varepsilon) = 1$ dB and then using (38), we obtain $G_{\mathrm{SINR}}(0.1T_c, 2.5) \approx 0.87$ dB and $G_{\mathrm{SINR}}(0.1T_c, 4) \approx 0.82$ dB. This example indicates that performance improvement can be achieved without unreasonable timing requirements.

It is now clear that the effect of timing error on the system performance is proportional to ε. By an appropriate choice of the constant C in the expression of $L(\varepsilon)$, one can reduce the effect of timing error on performance to a minimum. By calculating the rate of increase of $F_{BE}(\varepsilon, B)$ with various values of C when B equals the chip rate, we found that the highest rate of change can be achieved by choosing $C = 6.3$. This value of C is used in all numerical computations of the paper.

VI. Conclusions

In this paper, we have presented the analysis of a band-limited DS-CDMA system using WDF in the receiver. The WDF employed partially flattens the in-band cross-power spectrum of a pair of spreading and WDF's and hence helps to improve the system performance and increase the system capacity. When the system bandwidth is equal to the chip rate, numerical results show that the capacity of the proposed system with optimally tuned ε can be increased up to about 1 dB compared to the conventional system with $\varepsilon = 2$. It is further illustrated that the wider the system bandwidth available, the better the performance can be achieved by tuning the ε of the WDF employed. Finally, we have analyzed the sensitivity to timing error for the proposed receiver. Numerical computation shows that the increase in capacity presented in this paper is achievable without unreasonable timing tracking requirements.

References

[1] S. Verdú, "Minimum probability of error for asynchronous Gaussian multiple-access channels," *IEEE Trans. Inform. Theory*, vol. IT-32, pp. 85–96, Jan. 1986.

[2] Z. Xie, R. T. Short, and C. K. Rushforth, "A family of suboptimum detectors for coherent multiuser communications," *IEEE J. Select. Areas Commun.*, vol. 8, pp. 683–690, May 1990.

[3] M. Varanasi and B. Aazhang, "Multistage detection in asynchronous code-division multiple access communications," *IEEE Trans. Commun.*, vol. 38, pp. 509–519, Apr. 1990.

[4] Y. C. Yoon and H. Leib, "Matched filters with interference suppression capabilities for DS-CDMA," *IEEE J. Select. Areas Commun.*, vol. 14, pp. 1510–1521, Oct. 1996.

[5] A. Duel-Hallen, "A family of multiuser decision-feedback detectors for asynchronous code-division multiple-access channel," *IEEE Trans. Commun.*, vol. 43, pp. 421–434, Feb./Mar./Apr. 1995.

[6] A. Klein *et al.*, "Zero forcing and minimum mean-square-error equalization for multiuser detection in code-division multiple-access channels," *IEEE Trans. Veh. Technol.*, vol. 45, pp. 276–287, May 1996.

[7] A. M. Monk, M. Davis, L. B. Milstein, and C. H. Helstrom, "A noise-whitening approach to multiple access noise rejection—Part I: Theory and background," *IEEE J. Select. Areas Commun.*, vol. 12, pp. 817–827, June 1994.

[8] M. Davis, A. Monk, and L. B. Milstein, "A noise-whitening approach to multiple-access noise rejection—Part II: Implementation issues," *IEEE J. Select. Areas Commun.*, vol. 14, pp. 1488–1499, Oct. 1996.

[9] Y. Huang and T. S. Ng, "A DS-CDMA system using despreading sequences weighted by adjustable chip waveforms," *IEEE Trans. Commun.,* to be published.
[10] _____, "DS-CDMA with power control error using weighted despreading sequences over a multipath Rayleigh fading channel," *IEEE Trans. Veh. Technol.,* to be published.
[11] J. Viterbi, "Very low rate convolutional codes for maximum theoretical performance of spread-spectrum multiple access channels," *IEEE J. Select. Areas Commun.,* vol. 8, pp. 641–649, May 1990.
[12] L. Yu and J. E. Salt, "A hybrid spreading/despreading function with good SNR performance for band-limited DS-CDMA," *IEEE J. Select. Areas Commun.,* vol. 14, pp. 1576–1582, Oct. 1996.
[13] J. E. Salt and S. Kumar, "Effects of filtering on the performance of QPSK and MSK modulation in D-S spread spectrum systems using RAKE receivers," *IEEE J. Select. Areas Commun.,* vol. 12, pp. 707–715, May 1994.
[14] N. M. Blachman and S. H. Mousavinezhad, "The spectrum of the square of a synchronous random pulse train," *IEEE Trans. Commun.,* vol. 38, pp. 13–17, Jan. 1990.

Yuejin Huang (S'95–M'98) received the B.Sc. degree from the Sichuan University, China, in 1982, the M.Sc. degree from the Optics and Electronics Institute, Chinese Academy of Sciences, in 1988, and the Ph.D. degree from the University of Hong Kong, in 1988, all in electrical engineering.

From 1982 to 1985, he was employed as an Electrical Engineer by the Southwest Physics Institute of Chinese National Nuclear Corporation. From 1988 to 1994, he was a Member of Technical Staff at the Nanjing Astronomical Instruments Research Center, Chinese Academy of Sciences, where his interest was the analysis and design of control systems. During his Ph.D. studies at the University of Hong Kong (1994–1998), he was a Teaching and Research Assistant in the Department of Electrical and Electronic Engineering, conducting research in spread-spectrum communications. Currently, he is with McGill University, Montreal, Canada, working as a Postdoctoral Fellow in wireless communication systems. His research interests include spreading spectrum communications, signal processing, automatic control, and microprocessor-based instruments.

Tung-Sang Ng (S'74–M'78–SM'90), for photograph and biography, see p. 1091 of the July 1999 issue of this TRANSACTIONS.